




RESEARCH ARTICLE

Identification of new amoebae strains in rainbow trout (*Oncorhynchus mykiss*, Walbaum) farms affected by nodular gill disease (NGD) in Northeastern Italy

Ginevra Brocca^{1,2}  | Alessandro Truant³ | Hana Peckova⁴ | Martina Lisnerová⁴ | Alberto Perolo⁵  | Marialetizia Fioravanti⁶ | Ivan Fiala⁴ | Gianfranco Gabai¹ | Francesco Quaglio¹ | Andrea Gustinelli⁶ 

¹Department of Comparative Biomedicine and Food Science (BCA), University of Padova, Legnaro, Padua, Italy

²Aquatic Diagnostic Services, Atlantic Veterinary College, University of Prince Edward Island, Charlottetown, Prince Edward Island, Canada

³Department of Animal Medicine, Production and Health, University of Padova, Legnaro, Padua, Italy

⁴Institute of Parasitology, Biology Centre CAS, Ceske Budejovice, Czech Republic

⁵Servizio Tecnico Commerciale Aquafeed, Gruppo Veronesi, Verona, Veneto Region, Italy

⁶Department of Veterinary Medical Sciences, Alma Mater Studiorum University of Bologna, Ozzano dell'Emilia, Bologna, Italy

Correspondence

Ginevra Brocca, Aquatic Diagnostic Services, Atlantic Veterinary College, University of Prince Edward Island, 550 University Avenue, Charlottetown, PE C1A 4P3, Canada.
Email: gbrocca@upepei.ca

Funding information

Czech Science Foundation, Grant/Award Number: 19-28399X

Abstract

Nodular gill disease (NGD) is an emerging condition associated with amoeba trophozoites in freshwater salmonid farms. However, unambiguous identification of the pathogens still must be achieved. This study aimed to identify the amoeba species involved in periodic NGD outbreaks in two rainbow trout (*Oncorhynchus mykiss*) farms in Northeastern Italy. During four episodes (February–April 2023), 88 fish were euthanized, and their gills were evaluated by macroscopic, microscopic and histopathological examination. The macroscopic and microscopic severity of the lesions and the degree of amoebae infestation were scored and statistically evaluated. One gill arch from each animal was put on non-nutrient agar (NNA) Petri dishes for amoeba isolation, cultivation and subsequent identification with SSU rDNA sequencing. Histopathology confirmed moderate to severe lesions consistent with NGD and mild to moderate amoeba infestation. The presence of amoebae was significantly correlated with lesion severity. Light microscopy of cultured amoebae strains and SSU rDNA analysis revealed the presence of a previously characterized amoeba *Naegleria* sp. strain GERK and several new strains: two strains from Hartmannellidae, three vannellid amoebae from the genus *Ripella* and cercozoan amoeba *Rosculus*. Despite the uncertainty in NGD etiopathogenesis and amoebae pathogenic role, identifying known and new amoebae leans towards a possible multi-aetiological origin.

KEYWORDS

amphizoic amoeba, Italy, nodular gill disease (NGD), *Oncorhynchus mykiss*, rainbow trout, SSU rDNA

This is an open access article under the terms of the [Creative Commons Attribution-NonCommercial](https://creativecommons.org/licenses/by-nc/4.0/) License, which permits use, distribution and reproduction in any medium, provided the original work is properly cited and is not used for commercial purposes.

© 2024 The Authors. *Journal of Fish Diseases* published by John Wiley & Sons Ltd.

1 | INTRODUCTION

The rainbow trout (*Oncorhynchus mykiss*, Walbaum) is the most commonly farmed fish in Italy, with numerous facilities located near sources of cold and well-oxygenated water, such as the basins in the Northeastern part of the country. Numerous diseases affect production, and in recent years, severe gill lesions have been reported to be associated with amoebic parasite infestation, referable to the so-called nodular gill disease (NGD).

NGD is an emerging disease affecting freshwater salmonids worldwide. It was first described in rainbow trout in Canada (Daoust & Ferguson, 1985, 1986) and in the United States (Bullock et al., 1994). Since then, NGD episodes were reported also in Europe, Denmark (Buchmann et al., 2004), Poland (Antychowicz, 2007), Germany (Dyková et al., 2010), the Czech Republic (Dyková & Tyml, 2016), Italy (Quaglio et al., 2016), Spain (Bermúdez et al., 2019), Russia (Kudryavtsev et al., 2022) and Switzerland (Vannetti et al., 2023).

Rainbow trout is the most affected species, but outbreaks of NGD have also been reported in brown trout (*Salmo trutta*) (Perolo et al., 2019), chinook salmon (*Oncorhynchus tshawytscha*) (Tubbs et al., 2010), arctic char (*Salvelinus alpinus*) (Speare, 1999) and brook trout (*Salvelinus fontinalis*) (Perolo et al., 2018).

In Italy, the disease manifests from autumn to early spring, with greater severity in winter when the water temperature is under 12°C. The most affected animals are juveniles, around 20g, but sub-adult trout (around 100g) can be infected, and the cumulative mortality can reach 60% (Quaglio et al., 2016).

NGD outbreaks show many resemblances with the well-known amoebic gill disease (AGD) affecting saltwater salmonids and caused by *Neoparamoeba perurans* (Young et al., 2007).

Fish affected by NGD show severe respiratory distress, including surface swimming, ataxia and flared opercula. Macroscopically, the gills show excessive mucous production and a characteristic club-like appearance of filament tips, visible as multifocal to coalescent whitish nodules, indicative of severe epithelial hyperplasia. This can be better observed histologically as prominent respiratory epithelia proliferation producing extensive lamellar fusion with obliteration of the interlamellar space, mucous cell hypertrophy, lamellar oedema, necrosis and sloughing of epithelial cells. These changes contribute to the filaments' characteristic 'clubbing' (Speare & Ferguson, 2006).

The aetiological agent causing NGD has not been identified so far with certainty: *Thecamoeba hoffmani* (Buchmann et al., 2004; Sawyer et al., 1974), *Rhogostoma minus* (Dyková & Tyml, 2016), *Cochliopodium* sp. (Bermúdez et al., 2019; Daoust & Ferguson, 1985; Noble et al., 1997; Tubbs et al., 2010; Vannetti et al., 2023) and other amoebae from the genera *Acanthamoeba*, *Hartmannella* (now *Vermamoeba*), *Naegleria*, *Protacanthamoeba*, *Ripella*, *Saccamoeba*, *Mycamoeba* and *Vannella* (with recent isolation of *Vannella mustalhti* sp. nov. from Kudryavtsev et al., 2022) (Dyková et al., 2010; Jensen et al., 2020; Padrós & Constenla, 2021; Vannetti et al., 2023) have been proposed through the years. These findings support the hypothesis that a single agent might not cause the disease, which can be instead the result of multifactorial conditions that possibly involve multiple amoeba species.

Other factors, such as environmental conditions and concomitant infection from other pathological agents (e.g. bacteria), must be evaluated to clarify the etiopathogenesis of this condition and proceed toward a definitive assignment of disease causation through compliance with the Bradford Hill criteria and Koch's postulates.

In the present work, two Italian farms rearing rainbow trout and cyclically affected by NGD were monitored during the late winter and the beginning of spring 2021. The aim was to isolate and characterize the amoeba species possibly associated with the disease onset and to establish if a correlation existed between the abundance of amoebae and the severity of the lesions.

2 | MATERIALS AND METHODS

2.1 | Samples collection

The two rainbow trout farms in the Trentino region (Northeastern Italy) with suspected cases of NGD were monitored based on the reports by the trout farmers. The two farms are located on different riverwater basins: the Sarca River (farm A) and the Chiese River (farm B) (Figure 1). Samples were collected between February and April 2021. Fish were monitored for clinical signs of NGD, including lethargy, mortality and severe respiratory insufficiency (Antychowicz, 2007; Buchmann et al., 2004; Padrós & Constenla, 2021; Perolo et al., 2019; Quaglio et al., 2016). Environmental parameters (temperature, dissolved oxygen, water pH) and fish performance metrics (mean animal weight, animal rearing density and cumulative mortality) were collected for each sampling event. Moribund fish were euthanized by overdose of tricaine methanesulphonate (MS-222) anaesthetic solution (Pharmaq, Hampshire, UK) and immediately transported to the laboratory located within the farms for fresh mount examination and preliminary NGD diagnosis. Gills from positive fish were sampled and immediately put in 10% neutral-buffered formalin (NBF) or on non-nutrient agar (NNA) plates. They were then transported to the laboratories of the Department of Comparative Biomedicine and Food Science (BCA) of the University of Padua for histology, to the Department of Veterinary Medical Sciences for parasitological examination and to the Institute of Parasitology, Biological Centre of the Czech Academy of Science for amoebae cultivation, isolation and identification.

A total of 88 fish were collected over four samplings. Fourteen fish were collected in February 2021 from farm A, 18 fish, 22 fish and 34 fish were sampled from farm B over three samplings between February and April 2021.

2.2 | Macroscopic examination of the fish

A complete necropsy was performed on each animal selected for the analyses, visually examining the gill arches and the main organs (liver, spleen, kidney, heart and digestive tract). For the macroscopic evaluation of branchial arch hyperplasia status, a numerical score indicating the severity of the lesions was applied to each arch (Table 1, first

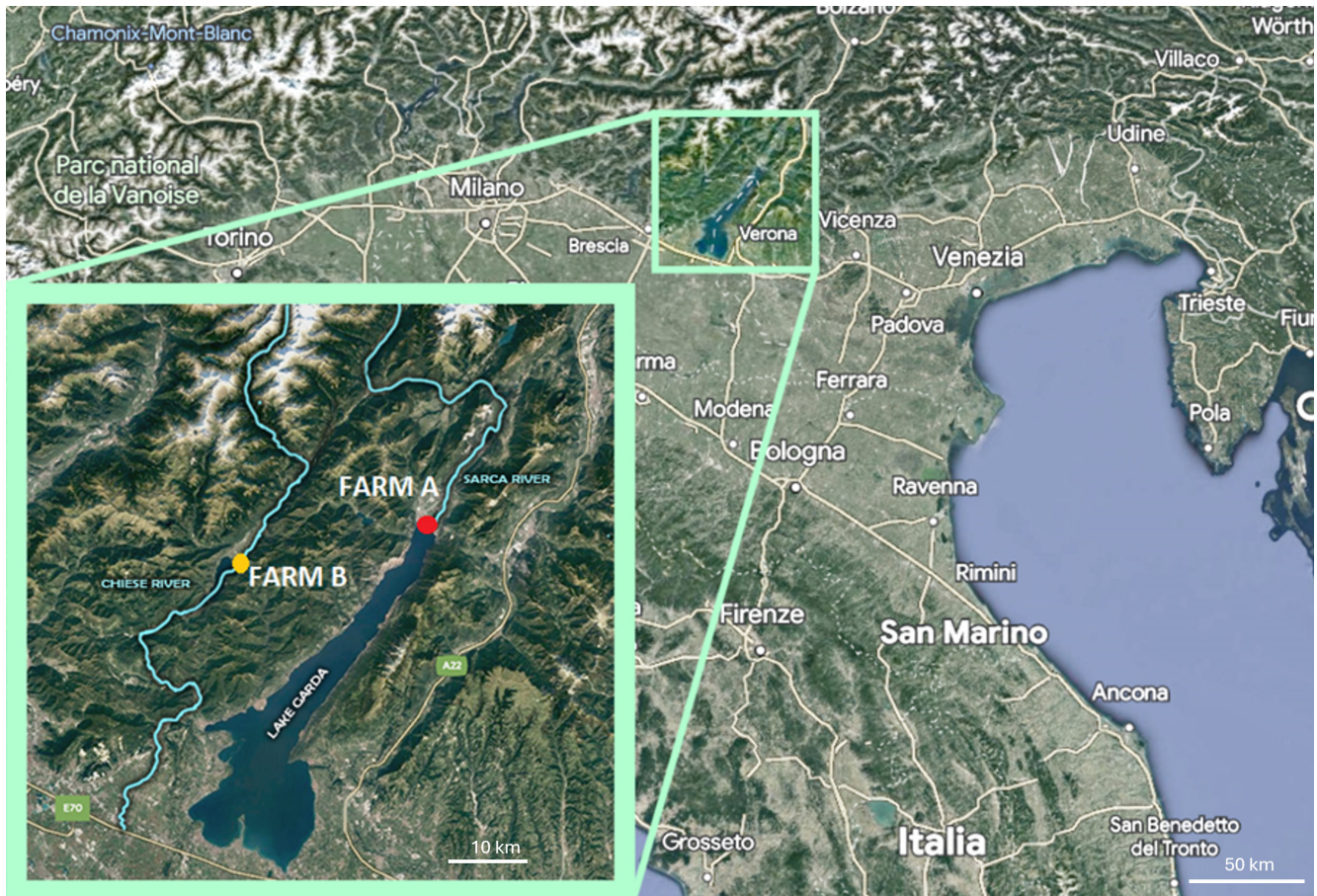


FIGURE 1 Map of the study highlighting the two sampling sites, farm A (red dot) and farm B (yellow dot).

column), modifying the classification method proposed for AGD evaluation of saltwater salmonids (Taylor et al., 2009) and more recently for NGD evaluation of rainbow trout (Vannetti et al., 2023), obtaining a macroscopic score (MaS) for each animal sampled in the study.

Once the MaS of each animal was scored accordingly, a gill macroscopic index (GMaI), calculated as the mean of all the MaS, was estimated for each NGD outbreak, as similarly done by Taylor et al. (2016). A mean index was also calculated, defined as the mean of all the individual MaS together, regardless of the sampling location.

2.3 | Fresh microscopic examination of the gills

From each animal's first right gill arch, a wet mount of gill scraping was obtained to evaluate and confirm the presence of amoebic trophozoites. The scrapes were evaluated in the in-farm laboratories with an optic microscope (Nikon Eclipse E100, 2015).

2.4 | Gill histopathology

Each animal's first left gill arch was sampled and fixed in 10% NBF for 48h, dehydrated in ethanol series and embedded in paraffin. Several sections were cut at 4 μ m and stained with haematoxylin and

eosin (HE), and Giemsa stainings, to better visualize trophozoites (Quaglio et al., 2016). Giemsa-stained slides were visualized with a Nikon Eclipse Ci-L (2011) optical microscope. Slides were evaluated to assess the severity of the hyperplastic reaction and the presence and distribution of the amoebae. The lesions' severity and the degree of amoebae infestation were scored numerically following the method proposed by Perolo et al. (2019) modified from Clark and Nowak (1999), obtaining a microscopic score (MiS) and an amoebic score (AS) (Table 1, second and third columns respectively). Once the MiS and AS of each animal were scored, a gill microscopic index (GMiI) and a gill amoebic index (GAI) were calculated for each outbreak as the mean of all the MiS and AS respectively.

Mean Indexes, defined as the mean of all the MiS and all the AS together, regardless of the sampling location, were also calculated.

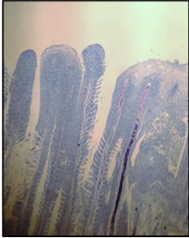
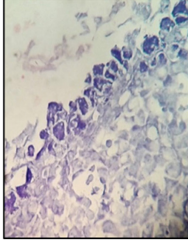
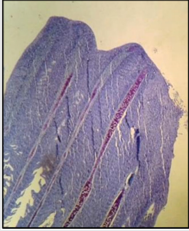
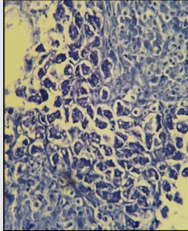
2.5 | Amoebae cultures maintenance, microscopic examination and molecular identification

A portion of the second left gill arch from each animal was put in NNA Petri dishes free from inactivated bacteria for the cultivation of cultures. The primary isolates obtained on day 10 post-inoculation were transferred to 1.5% nutrient agar containing malt nutrient agar with malt and yeast extracts with a few drops of PAGE solution

TABLE 1 Macroscopic (MaS), microscopic (MiS) and amoebic scores (AS) applied to estimate the severity of the lesions.

Score	Macroscopic (Mas)	Microscopic (MiS)	Amoebae (AS)
0, Null	Absence of lesions, the gills have a physiological red colour	Physiological aspect of filaments and lamellae, absence of any sign of tissue suffering or alteration	Complete absence of encysted or free amoebae
1, Very mild	Scattered focal area with mild proliferation and/or mild discoloration at the filament tips	Most filaments and lamellae have a physiological appearance; possible presence of a slight hyperplastic reaction in the apices of some filaments	Occasional presence of single amoebae, mainly encysted in the tissue surface
2, Mild	≤10% of gills showing mild proliferations and/or discolorations at the filament tips	The hyperplasia affects more than half of the filaments for a third of their length, with a club-like appearance	Small groups composed of 3–4 amoebae, free or encysted along the tissue surface
3, Moderate	10%–20% of gills showing proliferations of filament tips and thickening of the mucous layer	Gill arches with diffuse and modest epithelial proliferation affecting up to half the length of the filaments or branchial arches with few filaments affected by an intense hyperplastic reaction with fusion at the apical level; lamellar fusion, epithelial necrosis and mild to moderate goblet cells hyperplasia are frequent	Most hyperplastic filaments have groups with more than five amoebae, free or encysted along the tissue surface

TABLE 1 (Continued)

Score	Macroscopic (Mas)	Microscopic (MiS)	Amoebae (AS)
4, Severe	20%–50% of gills showing proliferations of filament tips and/or discoloration, with mucus patches	Most of the gill arch is affected by hyperplasia; the affected filaments show epithelial proliferation for more than two-thirds of their length and often there is a fusion of 3–4 filaments. In addition to sloughing and necrosis, there is marked hypertrophy of goblet cells	Continuous sequence of amoebae along the tissue surface of the hyperplastic filaments, with the possible presence of clusters of encysted amoebae
			
5, Very severe	>50% of gills affected by severe lesions	The hyperplastic reaction affects the entire gill arch; the affected filaments along their entire length are fused together in groups of five or more. Sloughing, necrosis and goblet cells hyperplasia are common	Numerous groups of amoebae that cover the filaments and occupy the inter-filamentary spaces and the pseudocysts formed by the fusion of lamellae and filaments
			

Note: MiS and AS were assessed by histological examination. MaS scoring system was modified from the classification method proposed for AGD evaluation of saltwater salmonids (Taylor et al., 2009, 2016) and NGD for rainbow trout (Vannetti et al., 2023). MiS and AS follow the method proposed by Perolo et al. (2019) and modified from Clark and Nowak (1999).

(Page, 1988) and then subcultured in Petri dishes with regular daily observation of the cultures. These agar plate cultures were maintained in an incubator at 15°C. None of the cultures were completely purified of accompanying bacteria, and no bacteria were added as food.

Petri dishes containing amoebae were washed using PAGE solution, and a drop of amoebae suspension was added to the cover slide. Amoebae were let to adhere for at least 30 min in a wet chamber. Then, the cover slide was used to observe amoebae in a hanging drop preparation using an Olympus BX51 (2000) light microscope equipped with Nomarski DIC optics and an Olympus DP71 digital camera.

Amoeba cultures were washed off agar plates, concentrated by centrifugation and resuspended in 400 µL TNES-urea buffer (10 mM Tris-HCl with pH8; 125 mM NaCl; 10 mM EDTA; 0.5% SDS and 4 M urea). Classic phenol-chloroform extraction (Sambrook et al., 1989) was used to obtain amoebae cultures DNA with overnight digestion with proteinase K (50 µg mL⁻¹; Serva, Germany) at 55°C. Extracted DNA was stored at -20°C.

PCRs were performed using an AccuPower® PCR PreMix (Bioneer, South Korea) containing 0.5 µL of each primer (25 pmol), 18 µL DNase-free water and 1 µL extracted DNA at a concentration of 50–200 ng/µL. Samples were prepared using the following primer combinations: (i) ERIB1 (5'-ACCTGGTTGATCCTGCCAG-3') and ERIB10 (5'-CTTCCGCAGGTTACACTACGG-3') (Barta et al., 1997) or (ii) 620F (5'-GCCAGCACCCGCGTAATCC-3') (Tymł et al., 2016) and ERIB10 (Barta et al., 1997). Primer pair ERIB1+ERIB10 amplifies almost complete SSU rDNA, whereas primer pair 620F+ERIB10 amplifies approximately 1500 bp. Cycle parameters were set as follows: Denaturation 95°C for 3 min, followed by 35 cycles of 94°C for 1 min, 58°C for 1 min, 72°C for 2 min with a terminal extension at 72°C for 10 min. PCR amplicons were extracted from the gel using the Gel/PCR DNA Fragments Extraction Kit (Geneaid Biotech Ltd., USA) and sequenced directly (SEQme, Czech Republic) using the Sanger method. Obtained PCR products with low band intensity or unclear sequencing results were cloned into the pDrive vector using a Qiagen PCR Cloning Kit (Qiagen, Germany) and transformed into competent *E. coli* cells. Plasmids were purified with a High Pure Plasmid Isolation Kit (Roche Applied Science,

Germany), and five plasmid clones were sequenced using the Sanger method (SEQme, Czech Republic). To determine the identity and phylogenetic relationships of amoebae strains, a BLAST search was first performed to identify SSU rDNA sequences with the highest similarity to the studied amoebae strains. Then, five individual alignments were prepared that included all available sequences of closely related amoebae available in GenBank. Nucleotide sequences were aligned using Mafft version 7.490 (Kato & Standley, 2013) implemented in Geneious Prime v 11.1 (Kearse et al., 2012), using the E-INS-I algorithm, with a gap opening penalty of 2.0. Maximum likelihood (ML) analyses were performed using RAxML v7.2.8 (Stamatakis, 2014) with the GTR+ Γ model of nucleotide substitution. Bootstrap supports were calculated from 1000 replicates. Strain-specific divergences were identified from proportional distances (in %) calculated in Geneious Prime based on the alignments used for the ML analysis.

2.6 | Statistical analysis

The data distribution between the two sampling sites was analysed using the Mann–Whitney nonparametric test.

The correlations among the diagnostic scores were expressed by Pearson's correlation coefficient (ρ), and the degree of agreement between the diagnostic classification criteria was assessed by Cohen's weighted kappa (κ).

Values between .1 and .3 were considered a weak correlation, between .4 and .6 moderate correlation and between .7 and .9 strong correlation.

The software IBM-SPSS Statistics 28.01 was used to perform the statistical analyses. The level of significance was set at $p < .05$.

3 | RESULTS

3.1 | Samples collection

All the fish collected exhibited clinical signs consistent with NGD, including lethargy, surface swimming, flared opercula and skin darkening.

The mean weight of the fish in both farms was 20–35 g, and the animals were raised with a 20 kg/m³ density. The cumulative mortality in both farmings and for all samplings reached 20%–30% over the sampling period. The water temperature remained stable, being 10–10.5°C in both farms, as well as the pH that was 7.5–8 in farm A and 7–8 in farm B. Dissolved oxygen concentration varied from 9 to 9.5 mg/L in farm A to 12 mg/L in farm B.

These water quality parameters remained constant in all four samplings in both farms over the sampling period examined.

3.2 | Macroscopic examination of fish

Macroscopically, the gills showed hypermucosity, alternated anaemic and congested areas and characteristic multifocal to coalescent

white nodules distributed along the filament distal extremities, referable to several adjacent filaments clubbed and fused (Figure 2). In the most severe cases, overgrowth of microorganisms referable to oomycetes of the genus *Saprolegnia* sp. was also observed. After opening the coelomic cavity, most subjects showed a brown discoloration of the liver, likely referable to prolonged hypoxia and hypercapnia. The other organs were unremarkable.

The MaS of each animal was scored and reported in Appendix S1; the mean indexes GMal for each sampling and the mean cumulative index are reported in Table 2.

Altogether, most of the gill arches had a moderate to severe level of macroscopic changes, and were assigned with higher frequency to MaS scores 3 and 4, with no entry registered for score 0 (Figure 3).

The GMal varied from 2.57 to 3.75, with a mean index of 3.50 among all the samplings.



FIGURE 2 Rainbow trout (*Oncorhynchus mykiss*). Pale nodules in the distal part of the filaments (arrowheads) referable to nodular gill disease (NGD).

TABLE 2 Gill macroscopic index (GMal), gill microscopic index (GMil) and gill amoebic index (GAI) were calculated for each sampling ($N = 4$) as the mean between all the calculated MaS, MiS and AS respectively. A mean index, reporting the mean of all the calculated scores, regardless of the outbreak location, is also provided.

Sampling	GMal	GMil	GAI
N. 1 (farm A) (n: 14)	2.57 ± 0.23	3.00 ± 0.23	1.14 ± 0.21
N. 2 (farm B) (n: 18)	3.72 ± 0.11	4.33 ± 0.14	2.44 ± 0.17
N. 3 (farm B) (n: 22)	3.50 ± 0.33	3.77 ± 0.23	2.41 ± 0.18
N. 4 (farm B) (n: 34)	3.75 ± 0.15	3.88 ± 0.13	2.65 ± 0.16
Mean index	3.50 ± 0.11	3.81 ± 0.10	2.31 ± 0.10

Note: Data are shown as mean ± SEM (standard error of the mean).

3.3 | Fresh microscopic examination of gills

When observed microscopically, the gill fresh mounts were characterized by a high number of alive amoebic trophozoites lining the gill surface or clustered between the lamellae. At 100× magnification, morphologically distinct subgroups of naked amoebae, with typical free pseudopods (Figure 4a) and testate amoebae, characterized by a shell-like structure (Figure 4b), were observed.

3.4 | Gill histopathology

The lesions observed in the 88 gill arches examined histologically revealed extensive hyperplasia of the respiratory epithelium, causing the rounding up of filaments extremities, obliteration of the interlamellar

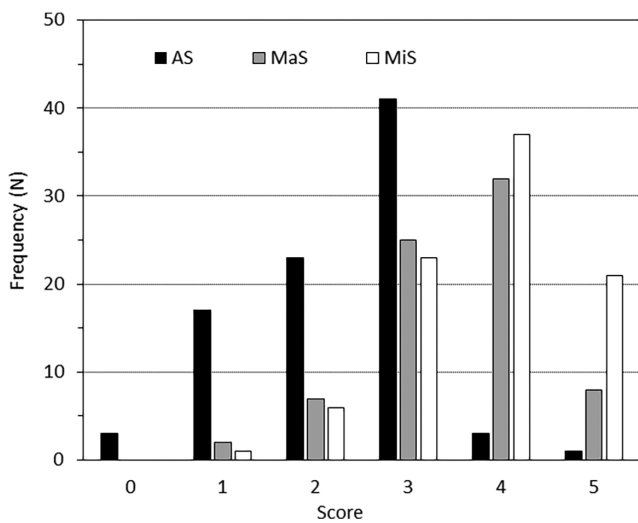


FIGURE 3 Observed score frequencies of the three diagnostic classifications (AS, amoebic score; MaS, macroscopic score; MiS, microscopic score) in sample farms A and B. The description of the scores is reported in Table 1.

spaces and fusion of adjacent filaments (Figure 5a). In the most severe cases, the filaments of the entire gill arch were fused together, causing a profound alteration of the gill architecture (Figure 5b). Other signs within the hyperplastic areas included spongiosis of the apical portions of the hyperplastic filaments (Figure 6a), lamellar oedema, necrosis and cellular sloughing of the respiratory epithelium, goblet cell hyperplasia and leucocyte infiltration of the filament axes (Figure 6b). In groups or single, numerous polyhedral amoebic elements with high Giemsa affinity were noted attached along the hyperplastic filaments (Figure 6c), encysted within the epithelial surface (Figure 6d), or within interlamellar pseudocysts (i.e. the space formed by apical fusion of adjacent lamellae) (Figure 6e). Trophozoites were characterized by a 15–25 μm diameter, one paracentral micronucleus, a clear perinuclear halo and numerous cytoplasmic basophilic to metachromatic granulations and vacuolizations (Figure 6f).

The scores of MiS and AS of each animal are reported in Appendix S1, the mean indexes GmiI and GAI for each sampling and the corresponding cumulative Mean Index are reported in Table 2.

Altogether, most specimens showed a moderate to severe hyperplastic disease (similar to macroscopic lesions) and were assigned with higher frequency to MiS scores 3, 4 and 5, with no entry registered for score 0 (Figure 3). The amoebic infestation was instead most frequently evaluated as mild to moderate, with a higher frequency of AS scores 1, 2 and 3 (Figure 3).

The GMiI varied from 3.00 to 4.33, with a mean index of 3.81 among all samplings. The GAI varied from 1.14 to 2.65, with a mean index of 2.31 among all the samplings.

3.5 | Amoebae morphological and molecular identification

Twelve primary amoebae isolates were obtained from 48 samples of gill arches showing signs of NGD and selected for amoebae

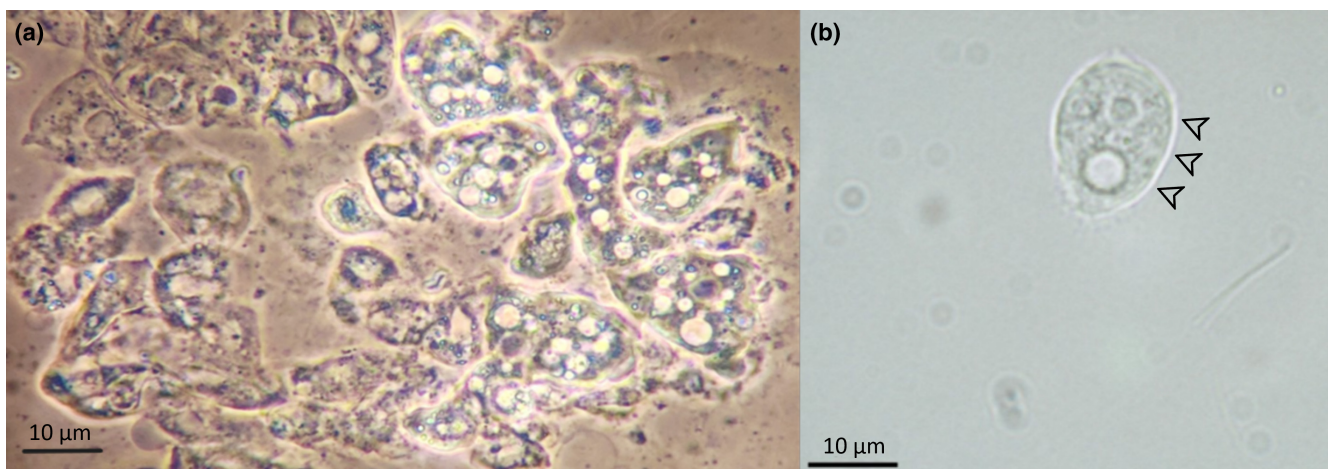


FIGURE 4 Gill fresh mounts showing the presence of naked amoebae (a) and testate amoeba (b). The arrowheads highlight the characteristic shell-like structure of testate amoebae (b).

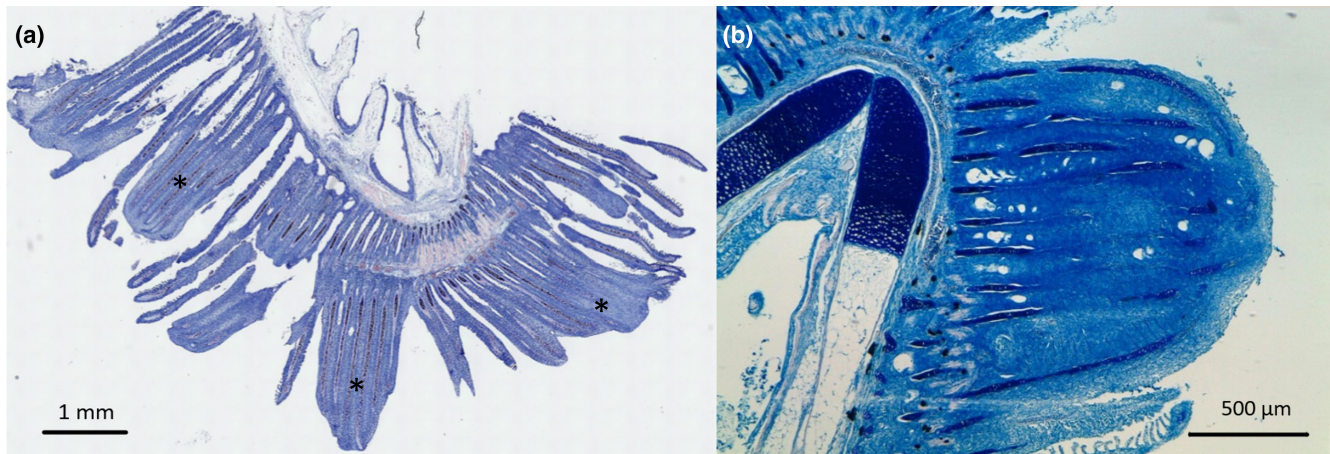


FIGURE 5 (a) Entire gill arch showing the microscopic alteration of the gill structure, characterized by hyperplasia of the respiratory epithelium with fusion of adjacent filaments (*) and lamellae, resulting in obliteration of the interlamellar spaces and classic club shape of the filaments, Giemsa stain. (b) Detail of severe alteration of the gill structure, involving an extensive portion of the gill arch and the fusion of approximately 10 filaments, Giemsa stain.

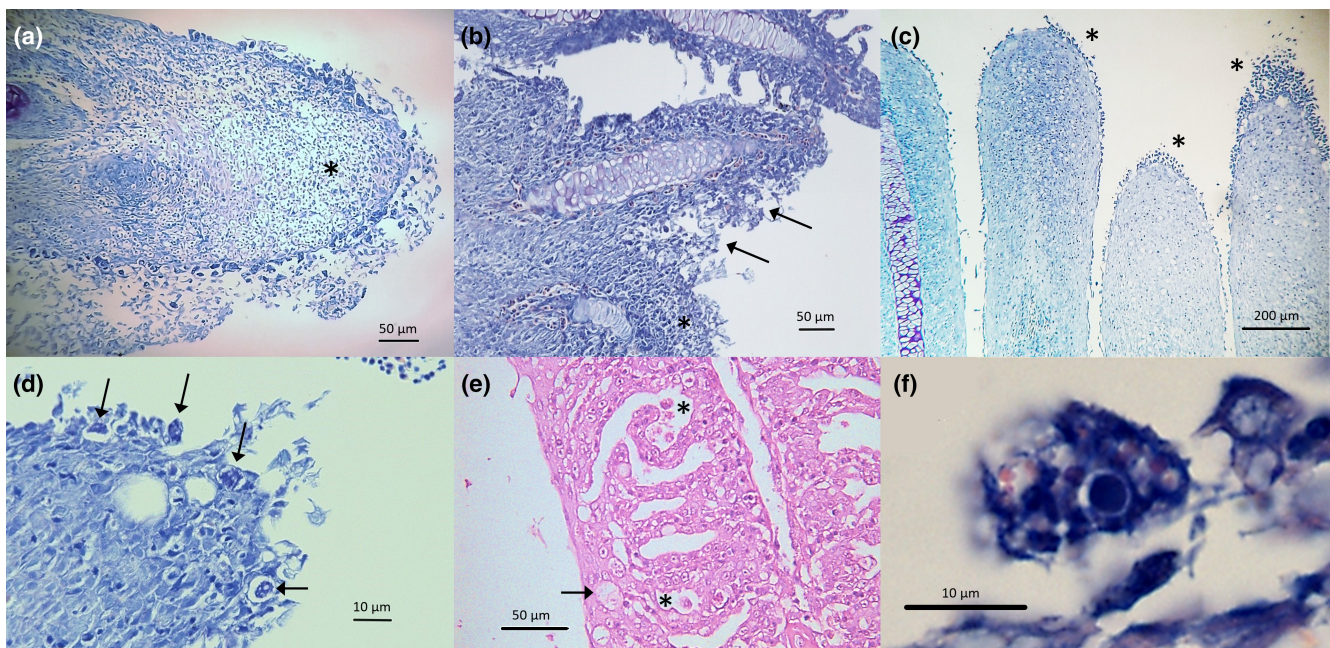


FIGURE 6 (a) The apex of the filament (*) shows prominent intercellular oedema (spongiosis), viewed as clear spaces within the gill epithelium, Giemsa stain. (b) Sloughing of respiratory epithelial cells (arrows) and leucocyte infiltration (*) of some gill filaments, Giemsa stain. (c) Apical hyperplasia of gill filaments showing clusters of trophozoites (*) along the surface. Trophozoites are characterized by intense Giemsa affinity, Giemsa stain. (d) Detail of amoeba trophozoites (arrows) encysted within the epithelial surface of the filament, Giemsa stain. (e) Presence of lacunae or pseudocysts (*) within the hyperplastic lamellae, containing cellular debris and trophozoites, and hypertrophic goblet cells (arrow), haematoxylin and eosin (HE). (f) Detail of a trophozoite with one paracentral micronucleus, a clear perinuclear halo and numerous cytoplasmic basophilic to metachromatic granulations and vacuolizations, Giemsa stain.

cultivation. Subsequent subculturing of these isolates resulted in cultures of five different strains. Based on morphology and phylogenetic analysis, these strains were assigned to the genus *Rosculus* (Figure 7a), *Copromyxa* (Figure 7b), *Ptolemeba* (Figure 7c), *Naegleria* (Figure 7d) and *Ripella* (Figure 7e). *Rosculus*, *Copromyxa* and *Ptolemeba* were only detected in samples from farm A isolated in February 2021, while *Ripella* amoebae were very abundant in all isolates from farm B isolated in April 2021 and were not detected

in isolates from farm A. *Rosculus* sp. strains were the most abundant amoebae in farm A and were present in four out of five primary isolates. *Naegleria* strains were the only ones detected in both farms.

All strains of *Rosculus*, the most abundant amoeba from farm A, were identical based on their SSU rDNA sequence and clustered in close relation to *Rosculus piscicus*. *Ptolemeba* sp. strain SARCA12B clustered together with all sequences of *Ptolemeba bulliensis* and

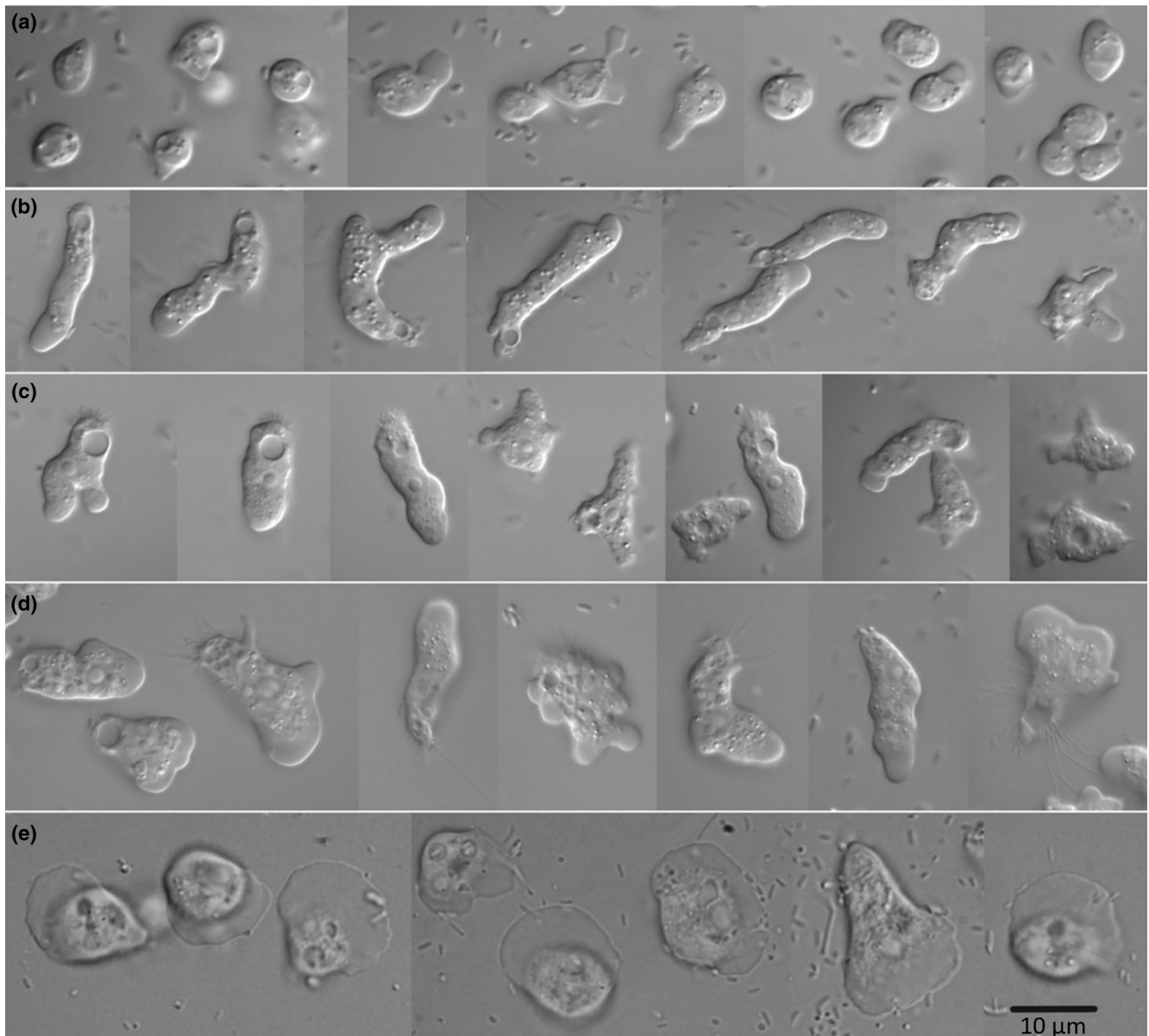


FIGURE 7 Differential interference contrast light photomicrographs of amoebae strains identified in NGD outbreaks. (a) *Rosculus* sp., (b) *Copromyxa* sp., (c) *Ptolemeba* sp., (d) *Naegleria* sp., (e) *Ripella* spp.

revealed more than 99% similarity with all of them. *Copromyxa* sp. strain SARCA3 was identified only in one primary isolate, and it clustered independently within *Copromyxa* species close to *Copromyxa cantabrigiensis* and *C. vandevyveri*.

Sequencing of *Ripella* isolates revealed they contained many morphologically indistinguishable but molecularly distinct *Ripella* strains. Due to their co-occurrence, we were able only to obtain three SSU rDNA sequences of these *Ripella* strains in good quality (strains CHIESE 83/1, CHIESE 83/2 and CHIESE 60). These three molecularly identified *Ripella* strains clustered independently, showing relatively high distance from each other (84%–94% similarity) and the other *Ripella* species and strains available in GenBank. Only the *Ripella* sp. strain CHIESE 83/1 was closely related to *Ripella* sp. GERL34 (GenBank [HM363631](#)). All three isolated *Naegleria* strains (represented by strain SARCA12) were identical to the strain

Naegleria sp. GERK (GenBank [HM363629](#)). The phylogenetic relationships of all strains are represented in [Figure 8](#). Sequences obtained in this study were deposited in GenBank under accession numbers PP258995–PP259001.

3.6 | Statistical analysis

The comparison of data distribution between Mas, MiS and AS revealed a statistically significant difference ($p = .001$) between Farm A and Farm B.

In farm A, the medians were 3.0 (1–4) for Mas, 3.0 (2–5) for MiS and 1.0 (0–3) for AS.

In farm B, the medians were 4.0 (2–5) for MaS, 4.0 (1–5) for MiS and 3.0 (0–5) for AS.

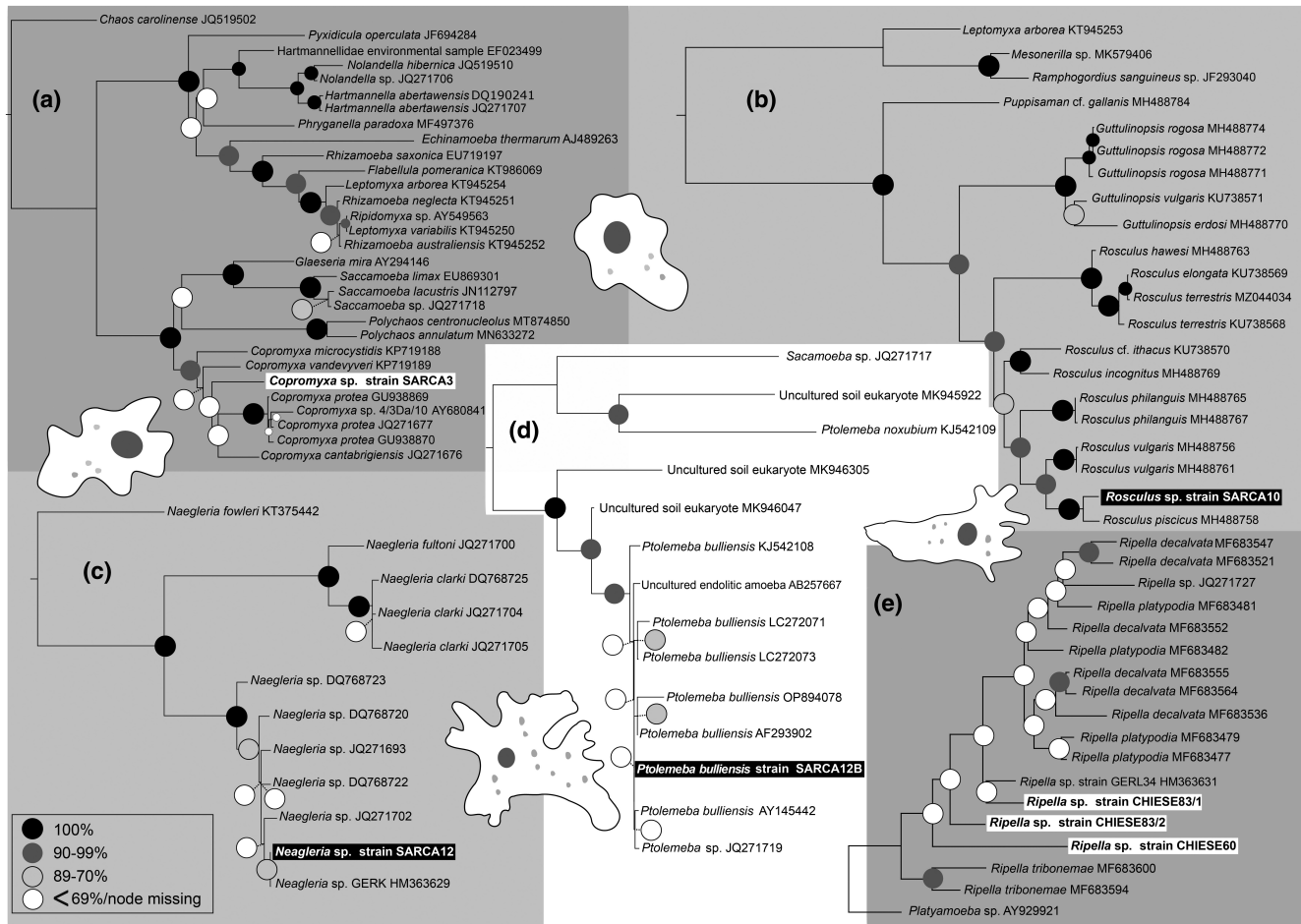


FIGURE 8 Maximum likelihood trees based on SSU rDNA sequences showing phylogenetic relationships of amoebae strains identified in NGD outbreaks. Bootstrap support values are indicated at each node. GenBank accession numbers of SSU sequences are listed next to the taxon names.

The statistical analysis also revealed the existence of a significant ($p < .001$) moderate correlation between the different scores: .614 between MaS and AS scores, .528 between MiS and AS scores and .465 between MaS and MiS scores. The accuracy was not significant between MaS and AS scores and significant but unremarkable for MaS-MiS and MiS-AS scores. The results are reported in [Table 3](#).

4 | DISCUSSION

This study represents one of the first attempts to overcome the anecdotal approach to the description of NGD in rainbow trout. Currently, most of the literature is based on case reports and descriptions of disease outbreaks. Although of considerable value, more in-depth studies are needed to establish the role of amoebae in this disease.

Given the high prevalence of rainbow trout farming systems in the Northeastern region of Italy and the high prevalence reported in the last decade of amoebic elements associated with hyperplastic

gill disease (Cocco et al., 2023), this area was selected as a starting point for a rigorous evaluation of the disease.

Notably, a statistical evaluation of the macroscopic and microscopic lesions associated with the intensity of amoebic infestation was performed and coupled with a strain identification that detected new and already reported amoebae strains, increasing the available dataset.

Even if some limiting factors must be considered, such as the different numerosity of the samplings (a frequent occurrence when field factors constrain research) and the wider sampling window for farm B, the two farms (which supply their water from two different river basins) showed an overall different amoeba profile and different severities of lesions, with farm B having a more severe level of amoebic infestation compared to farm A as testified by the higher GMaI, GMiI and GAI. This difference was also confirmed statistically by the non-parametric test. The higher scores in farm B may be associated with the numerous *Ripella* sp. strains, which were not present in farm A. However, this observation is not supported by statistical significance.

The histological evaluation confirmed the gill hyperplasia associated with the presence of amoebae. A general parallel trend between

TABLE 3 Weighted Cohen's Kappa (κ) test and Pearson correlation coefficients (ρ) between amoebic score (AS), macroscopic score (MaS) and microscopic score (MiS).

Comparison	N	κ	Z	p	ρ
AS vs. MiS	88	0.062 ± 0.026	2.418	.016	.528***
AS vs. MaS	74	0.137 ± 0.039	3.664	.000	.614***
MaS vs. MiS	74	0.343 ± 0.078	4.716	.000	.465***

***Indicates a highly significant correlation (ρ ; $p < .001$).

the severity of macroscopic lesions and the severity of gill hyperplasia and amoebic infestation was observed by the pathologists. There was a higher tendency to assign macroscopic and microscopic lesions to higher scores (3–5), while the evaluation of amoeba infestation was tentatively assigned to lower scores (1–3). This tendency is also reflected by the mean indexes, with GMal and GMil generally higher than GAI.

All the scores showed a moderate correlation between them, which was considered a satisfactory indicator of their consistency.

The correlation between MaS and MiS ($\rho = .465$) confirms that macroscopic lesions correspond to a similar histological alteration. The correlation between AS and MiS ($\rho = .528$) suggests that histological alterations are associated with a certain degree of amoebae proliferation on the gill tissue.

Whether this is of significance and could provide new insight into the etiopathogenesis of the disease is still a matter of debate.

Despite the moderate correlation between all the scoring systems applied, Cohen's Kappa analysis showed low agreement between assigned values. This is probably due to the data dispersion, which could be explained by the high number of classes used for pathology scoring (0–5). For future analysis, using fewer classes would potentially increase the reliability of the data, allowing for a better practical value of the scoring system.

A mean index was also calculated for each type of score. Of the three, the GMal is the only one that can potentially be performed on the field and represents a cost-effective tool that allows a non-invasive, real-time evaluation of gross gill lesions in fish with clinical signs of NGD, useful for farm management decisions. However, it is based on a subjective evaluation and does not allow to assess the degree of amoeba infestation. More likely, the index is strictly correlated to gill hyperplasia.

GMil and GAI are invasive and time-consuming but allow an accurate qualitative and semi-quantitative evaluation of gill lesions and amoebic infestation and the comparison of pathological development at different time points, places and fish groups.

Of the seven amoebae strains identified in NGD outbreaks in the Italian farms, only one has been reported before in NGD salmonid outbreaks (Dyková et al., 2010). Strain SARCA12 was found identical to *Naegleria* sp. GERK (Genbank: [HM363629](#)), detected in rainbow trout in southeastern Germany. Strain SARCA12 is likely almost identical to isolate K77_3F5 detected in rainbow trout in Switzerland (Vannetti et al., 2023), deduced from the given high sequence similarity of K77_3F5 and *Naegleria* sp. GERK, but the direct comparison could not be made due to unpublished sequence data for K77_3F5. Similarly to the study of Vannetti et al. (2023), three strains of the genus *Ripella* were identified. Their sequences could not be compared due to unpublished sequence data of

Ripella amoebae in Vannetti et al. (2023). *Ripella* strains identified in our study clustered separately without close relation to known *Ripella* sequences except for strain CHIESE83/1, showing close relation to *Ripella* sp. strain GERL34 ([HM363631](#)) that was described as *Vannella* sp. in Dyková et al. (2010), the same study on NGD outbreak in southeastern Germany. This suggests a potential link between the NGD outbreak in Italian farms and the outbreak described by Dyková et al. (2010). However, none of the other seven amoebae strains identified in their study and classified into genera *Acanthamoeba*, *Hartmannella*, *Protacanthamoeba* and *Vannella* have been detected in our study. Moreover, the three remaining strains identified in our study were not reported in Dyková et al. (2010).

The strain SARCA12B was found to be *Ptolemya bulliensis*. It showed a close relationship and more than 99% similarity in its SSU rDNA with several *P. bulliensis* strains, including LOS7N/I ([AY145442](#)), which was isolated from the gills of Atlantic salmon caught in the Elbe River in the Czech Republic (Dyková et al., 2002). The almost identical SSU rDNA sequences and indistinguishable morphology of these two strains suggest that *P. bulliensis* can infect rainbow trout and Atlantic salmon. Strain SARCA3 has been classified in the genus *Copromyxa*, showing a close relation to *C. protea* and *C. cantabrigiensis*, never reported from fish tissues. Interestingly, strain SARCA10 clustered within cercozoan *Rosculus* spp. with a close relation to *R. piscicus* isolated from the gut content of green sunfish (*Lepomis cyanellus*) (Schuler et al., 2018).

The isolated amoebae differed between the two farms except for *Naegleria* sp., which was found in both. The same amoeba was also present in NGD outbreaks in rainbow trout in southeastern Germany (Dyková et al., 2010), supporting that this amoeba is a potential aetiological agent in NGD outbreaks. Similarly, identifying a *Ripella* strain closely resembling the one detected in an outbreak in Southeastern Germany raises *Ripella* as a potential agent in NGD, even if it was only detected in farm B. Nevertheless, our results are in accordance with the hypothesis that different amoebae are possibly implied in NGD outbreaks.

However, this can be explained by the difficulty of isolating and cultivating amoebae. It is already well-known that cultivation-based methods imply a selective bias for amoebae able to grow in artificial media. It has been estimated that more than 99% of bacterial and archeal species have not been cultured yet, being part of the so-called Microbial Dark Matter (Jiao et al., 2021; Yarza et al., 2014).

Moreover, morphological identification of naked lobose amoeba is difficult and often inadequate, and many species with high morphological similarity have genetic differences. Until now, the main phylogenetic studies on Amoebozoa organisms are based on the

sequencing of the SSU rRNA gene, resulting in an extensive database of this marker and enabling species comparison and identification. As reported by Nasonova et al. (2010), the COI gene (Cytochrome C Oxidase subunit I gene) and ITS (Internal Transcribed Spacer) region provide better resolution for taxonomic identification and polymorphism individuation into the same species. However, very few data are available compared with SSU rRNA gene analysis. For precise species identification, including taxonomic analysis using the COI gene and ITS region in future studies will be helpful.

The upcoming analyses will be focused on the ultrastructural evaluation of amoebae trophozoites with TEM (Transmission Electron Microscopy) to obtain a precise description of organelles and cellular structures, such as mitochondrial cristae, nucleus and cellular membrane. This information can be paired with genetic analysis to obtain more accurate identification, classification and new species description, particularly in the case of *Naegleria* sp. that we identified more frequently associated with NGD.

Overall, the evaluation of the possible pathogenic role of different amoeba species has proven to be challenging, and the application of rigorous histopathological and cultivation methods has shown how different farms are characterized by different amoebic populations. In this regard, *Naegleria* represents the only common factor between the two sites. However, further studies are needed to fulfil the Bradford Hill criteria and Koch's postulate to assign disease causation in NGD.

Specifically, more studies will have to focus on the complex relationship between amoebae and gill respiratory epithelium. Gills have a stereotypical response to many noxious stimuli, and determining the initial stimulating injury can be challenging. Moreover, many factors other than pathogens contribute to establishing a disease (Cocco et al., 2023), including water temperature, population density, environmental contaminant, stress and fish development stage (Adams & Nowak, 2001; Zilberg & Munday, 2000).

Currently, the available data only prove a correlation between the damage and the amoebic infestation; however, known factors capable of inducing gill hyperplasia include filamentous bacteria, organic material in the water (which amoebae feed on) and suspended solids. All these factors are also recognized as predisposing conditions for amoebae growth (Dyková & Tým, 2016; Lasjerdi et al., 2011; Loret & Greub, 2010). Whether amoebae are present in NGD cases as opportunistic pathogens, as a component of a multifactorial disease starring multiple amoeba species and other microorganisms and even environmental conditions, or as a primary pathogen is still unknown.

For a better understanding of the correlation and causation between tissue lesions and the presence of amoebae, it will be necessary to observe the progression of the pathology thoroughly (Clark & Nowak, 1999; Zilberg & Munday, 2000). However, comparing macroscopic and microscopic aspects with the presence of amoebae is challenging at the initial stage of the pathology due to the absence of visible lesions and clinical symptoms that indicate the rise and development of the disease.

In the future, only experimental infection trials will be able to prove a causative relationship and describe the initial stages of the disease.

Of great interest for future studies is the investigation of the amoeba population profiles in association with other environmental factors and with other pathogens, both during periods not characterized by disease and during disease peaks. For such kinds of studies, the investigation of amoeba population profiles through next-generation sequencing (NGS) techniques is being developed more and more. The NGS sequencing of the 18S rRNA gene permits the simultaneous screening of all the eukaryotic populations in each sample. This would allow us to monitor the different amoeba populations and better elucidate the disease trend in the field and the involvement of amoeba in its progression. These techniques are already applied in Atlantic salmon affected by AGD (Birlanga et al., 2022), and their potential for rainbow trout also seems promising.

In conclusion, this research allowed the characterization of amoeba strains associated with NGD outbreaks in rainbow trout in Trentino fish farms. The isolated amoeba species confirmed the presence of *Naegleria* spp., a species that has already been detected in other NGD outbreaks, as well as new species belonging to the genera *Rosculus* sp., *Copromyxa* sp. and *Ptolemya* sp. that have never been described before in other NGD outbreaks, neither in Italy nor in other European or non-European countries. These data strengthen the hypothesis that NGD is a multi-aetiological disease. Future metagenomic and infection tests will be necessary to confirm the pathogenic role of the identified species in the onset and progression of the pathology, as well as to determine whether they are saprophytic, commensal, opportunistic, or primary agents of the disease.

The correlation between macroscopic evaluation of gill alterations, microscopic assessment of lesions and amoeba infestation level has been assessed, confirming the practicality of these scoring systems and their reliability in quantifying tissue damage at the gill level.

AUTHOR CONTRIBUTIONS

Ginevra Brocca: Investigation; writing – original draft; methodology; writing – review and editing. **Alessandro Truant:** Investigation; writing – original draft; writing – review and editing; methodology. **Hana Peckova:** Methodology; formal analysis. **Martina Lisnerová:** Methodology; formal analysis. **Alberto Perolo:** Visualization. **Marialetizia Fioravanti:** Supervision. **Ivan Fiala:** Formal analysis; software; writing – review and editing; methodology; investigation; funding acquisition; conceptualization. **Gianfranco Gabai:** Data curation; supervision. **Francesco Quaglio:** Conceptualization; investigation; funding acquisition; writing – original draft; writing – review and editing; supervision; project administration. **Andrea Gustinelli:** Conceptualization; investigation; writing – original draft; writing – review and editing; supervision; project administration.

ACKNOWLEDGEMENTS

The authors acknowledge the farmers for providing the case material.

FUNDING INFORMATION

This study was supported by internal resources of the BCA Department and by the Czech Science Foundation (project# 19-28399X).

CONFLICT OF INTEREST STATEMENT

The authors declare no conflict of interest.

DATA AVAILABILITY STATEMENT

All data generated or analysed are included in the article. All materials are available from the corresponding author, on request. The sequences obtained in this study were deposited in GenBank under accession numbers PP258995-PP259001.

ORCID

Ginevra Brocca  <https://orcid.org/0000-0002-3531-1592>

Alberto Perolo  <https://orcid.org/0000-0002-0460-1327>

Andrea Gustinelli  <https://orcid.org/0000-0002-4249-4278>

REFERENCES

- Adams, M. B., & Nowak, B. F. (2001). Distribution and structure of lesions in the gills of Atlantic salmon, *Salmo salar* L., affected with amoebic gill disease. *Journal of Fish Diseases*, 24, 535–542. <https://doi.org/10.1046/j.1365-2761.2001.00330.x>
- Antychowicz, J. (2007). Study on rainbow trout nodular gill disease detected in Poland. *Bulletin of the Veterinary Institute in Pulawy*, 51, 547–551.
- Barta, J. R., Martin, D. S., Liberator, P. A., Dashkevich, M., Anderson, J. W., Feighner, S. D., Elbrecht, A., Perkins-Barrow, A., Jenkins, M. C., Danforth, H. D., Ruff, M. D., & Profous-Juchelka, H. (1997). Phylogenetic relationships among eight *Eimeria* species infecting domestic fowl inferred using complete small subunit ribosomal DNA sequences. *The Journal of Parasitology*, 83, 262–271. <https://doi.org/10.2307/3284453>
- Bermúdez, R., Losada, A., De Azevedo, A. M., Castrillo, P. A., Ronza, P., Rubiolo, J. A., Sotelo, M., & Quiroga, M. I. (2019). Nodular gill disease in rainbow trout, an emerging disease? 19th International Conference on Diseases of Fish and Shellfish. Abstract Book, 147.
- Birlanga, V. B., McCormack, G., Ijaz, U. Z., MacCarthy, E., Smith, C., & Collins, G. (2022). Dynamic gill and mucus microbiomes during a gill disease episode in farmed Atlantic salmon. *Scientific Reports*, 12, 1–13. <https://doi.org/10.1038/s41598-022-17008-2>
- Buchmann, K., Nielsen, T., Sigh, J., & Bresciani, J. (2004). Amoebic gill infections of rainbow trout in freshwater ponds. *Bulletin of the European Association of Fish Pathologists*, 24, 87–91.
- Bullock, G., Herman, R., Heinen, J., Noble, A., Weber, A., & Hankins, J. (1994). Observations on the occurrence of bacterial gill disease and amoeba gill infestation in rainbow trout cultured in a water recirculation system. *Journal of Aquatic Animal Health*, 6, 310–317. [https://doi.org/10.1577/1548-8667\(1994\)006<0310:OOTOOB>2.3.CO;2](https://doi.org/10.1577/1548-8667(1994)006<0310:OOTOOB>2.3.CO;2)
- Clark, A., & Nowak, B. F. (1999). Field investigations of amoebic gill disease in Atlantic salmon, *Salmo salar* L., in Tasmania. *Journal of Fish Diseases*, 22, 433–443. <https://doi.org/10.1046/j.1365-2761.1999.00175.x>
- Cocco, A., Toson, M., Perolo, A., Casarotto, C., Franzago, E., Brocca, G., Verin, R., Quaglio, F., Dalla Pozza, M., & Bille, L. (2023). Nodular gill disease in Northeastern Italy: An investigation on the prevalence of the disease and the risks of introduction in rainbow trout farms. *Journal of Fish Diseases*, 46, 1021–1028. <https://doi.org/10.1111/jfd.13821>
- Daoust, P. Y., & Ferguson, H. W. (1985). Nodular gill disease: A unique form of proliferative gill disease in rainbow trout, *Salmo gairdneri* Richardson. *Journal of Fish Diseases*, 8, 511–522. <https://doi.org/10.1111/j.1365-2761.1985.tb00966.x>
- Daoust, P. Y., & Ferguson, H. W. (1986). Potential for recovery in nodular gill disease of rainbow trout, *Salmo gairdneri* Richardson. *Journal of Fish Diseases*, 9, 313–318. <https://doi.org/10.1111/j.1365-2761.1986.tb01020.x>
- Dyková, I., Kostka, M., Wortberg, F., Nardy, E., & Pecková, H. (2010). New data on aetiology of nodular gill disease in rainbow trout, *Oncorhynchus mykiss*. *Folia Parasitologica (Praha)*, 57, 157–163. <https://doi.org/10.14411/fp.2010.021>
- Dyková, I., & Tým, T. (2016). Testate amoeba *Rhogostoma minus* Belar, 1921, associated with nodular gill disease of rainbow trout, *Oncorhynchus mykiss* (Walbaum). *Journal of Fish Diseases*, 39, 539–546. <https://doi.org/10.1111/jfd.12384>
- Dyková, I., Veverková, M., Fiala, I., & Macháčková, B. (2002). A free-living amoeba with unusual pattern of mitochondrial structure isolated from Atlantic salmon, *Salmo salar* L. *Acta Protozoologica*, 41, 415–419. <https://doi.org/10.1111/jfd.12384>
- Jensen, H. M., Karami, A. M., Mathiessen, H., Al-Jubury, A., Kania, P. W., & Buchmann, K. (2020). Gill amoebae from freshwater rainbow trout (*Oncorhynchus mykiss*): In vitro evaluation of antiparasitic compounds against *Vannella* sp. *Journal of Fish Diseases*, 43, 665–672. <https://doi.org/10.1111/jfd.13162>
- Jiao, J. Y., Liu, L., Hua, Z. S., Fang, B. Z., Zhou, E. M., Salam, N., Hedlund, B. P., & Li, W. J. (2021). Microbial dark matter coming to light: Challenges and opportunities. *National Science Review*, 8, nwaa280. <https://doi.org/10.1093/nsr/nwaa280>
- Katoh, K., & Standley, D. M. (2013). MAFFT multiple sequence alignment software version 7: Improvements in performance and usability. *Molecular Biology and Evolution*, 30, 772–780. <https://doi.org/10.1093/molbev/mst010>
- Kearse, M., Karami, A. M., Mathiessen, H., Al-Jubury, A., Kania, P. W., & Buchmann, K. (2012). Geneious basic: An integrated and extendable desktop software platform for the organization and analysis of sequence data. *Bioinformatics*, 28, 1647–1649. <https://doi.org/10.1093/bioinformatics/bts199>
- Kudryavtsev, A., Parshukov, A., Kondakova, E., & Volkova, E. (2022). *Vannellamustalahtiana* sp. nov. (Amoebozoa, Vannellida) and rainbow trout nodular gill disease (NGD) in Russia. *Diseases of Aquatic Organisms*, 148, 29–41. <https://doi.org/10.3354/dao03641>
- Lasjerdi, Z., Niyiyati, M., Haghghi, A., Zaeri, F., & Nazemalhosseini Mojarad, E. (2011). First report of Vannellidae amoebae (*Vannella* spp.) isolated from biofilm source. *Iranian Journal of Parasitology*, 6, 84–89.
- Loret, J.-F., & Greub, G. (2010). Free-living amoebae: Biological bypasses in water treatment. *International Journal of Hygiene and Environmental Health*, 213, 167–175. <https://doi.org/10.1016/j.ijheh.2010.03.00418>
- Nassonova, E., Smirnov, A., Fahrni, J., & Pawlowski, J. (2010). Barcoding amoebae: Comparison of SSU, ITS and COI genes as tools for molecular identification of naked Lobose amoebae. *Protist*, 161, 102–115. <https://doi.org/10.1016/j.protis.2009.07.003>
- Noble, A. C., Herman, R. L., Noga, E. J., & Bullock, G. L. (1997). Recurrent amoebic gill infestation in rainbow trout cultured in a semiclosed water recirculation system. *Journal of Aquatic Animal Health*, 9, 64–69. [https://doi.org/10.1577/1548-8667\(1997\)009<0064:RAGIIR>2.3.CO;2](https://doi.org/10.1577/1548-8667(1997)009<0064:RAGIIR>2.3.CO;2)
- Padrós, F., & Constenla, M. (2021). Diseases caused by amoebae in fish: An overview. *Animals*, 11, 991. <https://doi.org/10.3390/ani11040991>
- Page, F. C. (1988). A New Key to Freshwater and Soil Gymnamoebae. *Freshwater Biological Association, Cumbria* (p. 122).
- Perolo, A., Gustinelli, A., Fioravanti, M. L., Manfrin, A., Dalla Pozza, M., Lunelli, F., Accini, A., & Quaglio, F. (2019). Occurrence of nodular gill disease in farmed brown trout (*Salmo trutta* L.). *Journal of Fish Diseases*, 42, 1315–1320. <https://doi.org/10.1111/jfd.13027>
- Perolo, A., Manfrin, A., Dalla, P. M., Pretto, T., Gustinelli, A., Fioravanti, M. L., & Quaglio, F. (2018). Prime osservazioni di malattia nodulare branchiale nel salmerino di fonte (*Salvelinus fontinalis*). Atti del XXIII Convegno Nazionale della Società Italiana di Patologia Ittica. Torino, 11–13 ottobre 2018 Castello del Valentino. Libro degli Abstract (p. 27).

- Quaglio, F., Perolo, A., Bronzatti, P., Gustinelli, A., Menconi, V., Cavazza, G., Caffara, M., Manfrin, A., Gallo, E., & Fioravanti, M. L. (2016). Nodular gill disease in farmed rainbow trout (*Oncorhynchus mykiss*) in Italy. *Journal of Fish Diseases*, 39, 1139–1142. <https://doi.org/10.1111/jfd.12446>
- Sambrook, J., Fritsch, E. F., & Maniatis, T. (1989). *Molecular cloning: A laboratory manual* (2nd ed., p. 626). Cold Spring Harbor Press.
- Sawyer, T. K., Hnath, J. G., & Conrad, J. F. (1974). *Thecamoeba hoffmani* sp. n. (Amoebida: Thecamoebidae) from gills of fingerling salmonid fish. *Journal of Parasitology*, 60, 677–682.
- Schuler, G. A., Tice, A. K., Pearce, R. A., Foreman, E., Stone, J., Gammill, S., & Brown, M. W. (2018). Phylogeny and classification of novel diversity in Sainouroidea (Cercozoa, Rhizaria) sheds light on a highly diverse and divergent clade. *Protist*, 169, 853–874. <https://doi.org/10.1016/j.protis.2018.08.002>
- Speare, D. J. (1999). Nodular gill disease (amoebic gill infestation) in Arctic char, *Salvelinus alpinus*. *Journal of Comparative Pathology*, 121, 277–282. <https://doi.org/10.1053/jcpa.1999.0317>
- Speare, D. J., & Ferguson, H. W. (2006). Gills and pseudobranchs. In H. W. Ferguson (Ed.), *Systemic pathology of fish* (2nd ed., p. 51). Scotian Press.
- Stamatakis, A. (2014). RAxML version 8: A tool for phylogenetic analysis and post-analysis of large phylogenies. *Bioinformatics*, 30, 1312–1313. <https://doi.org/10.1093/bioinformatics/btu033>
- Taylor, R. S., Huynh, H., Cameron, D., Evans, B., Cook, M., & Ritchie, G. (2016). Gill Score Guide Amoebic Gill Disease (AGD) Management Training Document. Hobart, Australia: Tassal Operations Pty.
- Taylor, R. S., Muller, W. J., Cook, M. T., Kube, P. D., & Elliott, N. G. (2009). Gill observations in Atlantic salmon (*Salmo salar*, L.) during repeated amoebic gill disease (AGD) field exposure and survival challenge. *Aquaculture*, 290, 1–8. <https://doi.org/10.1016/j.aquaculture.2009.01.030>
- Tubbs, L., Wybourne, B. A., Lumsden, J. S., & Lumsden, J. S. (2010). Nodular gill disease causing proliferative branchitis and mortality in chinook salmon (*Oncorhynchus tshawytscha*). *New Zealand Veterinary Journal*, 58, 59–61. <https://doi.org/10.1080/00480169.2010.65061>
- Tyml, T., Lares-Jiménez, L. F., Kostka, M., & Dyková, I. (2016). *Neovahlkampfia nana* n. sp. reinforcing an underrepresented subclade of Tetramitia, Heterolobosea. *Journal of Eukaryotic Microbiology*, 64, 78–87. <https://doi.org/10.1111/jeu.12341>
- Vannetti, S. M., Wynne, J. W., English, C., Huynh, C., Knüsel, R., de Sales-Ribeiro, C., Widmer, M., Delalay, G., & Schmidt-Posthaus, H. (2023). Amoeba species colonizing the gills of rainbow trout (*Oncorhynchus mykiss*) in Swiss aquaculture. *Journal of Fish Diseases*, 46, 987–999. <https://doi.org/10.1111/jfd.13819>
- Yarza, P., Yilmaz, P., Pruesse, E., Glöckner, F. O., Ludwig, W., Schleifer, K. H., Whitman, W. B., Euzéby, J., Amann, R., & Rosselló-Móra, R. (2014). Uniting the classification of cultured and uncultured bacteria and archaea using 16S rRNA gene sequences. *Nature Reviews Microbiology*, 12, 635–645. <https://doi.org/10.1038/nrmicro3330>
- Young, N. D., Crosbie, P. B. B., Adams, M. B., Nowak, B. F., & Morrison, R. N. (2007). *Neoparamoeba perurans* n. sp., an agent of amoebic gill disease of Atlantic salmon (*Salmo salar*). *International Journal for Parasitology*, 37, 1469–1481. <https://doi.org/10.1016/j.ijpara.2007.04.018>
- Zilberg, D., & Munday, B. L. (2000). Pathology of experimental amoebic gill disease in Atlantic salmon, *Salmo salar* L., and the effect of pre-maintenance of fish in sea water on the infection. *Journal of Fish Diseases*, 23, 401–407. <https://doi.org/10.1046/j.1365-2761.2000.00252.x>

SUPPORTING INFORMATION

Additional supporting information can be found online in the Supporting Information section at the end of this article.

How to cite this article: Brocca, G., Truant, A., Peckova, H., Lisnerová, M., Perolo, A., Fioravanti, M., Fiala, I., Gabai, G., Quaglio, F., & Gustinelli, A. (2024). Identification of new amoebae strains in rainbow trout (*Oncorhynchus mykiss*, Walbaum) farms affected by nodular gill disease (NGD) in Northeastern Italy. *Journal of Fish Diseases*, 00, e13933. <https://doi.org/10.1111/jfd.13933>